



# CT abnormalities evocative of lung infection are associated with lower $^{18}\text{F}$ -FDG uptake in confirmed COVID-19 patients

Achraf Bahloul<sup>1</sup> · Caroline Boursier<sup>1</sup> · Hélène Jeulin<sup>2</sup> · Laëtitia Imbert<sup>1,3</sup> · Damien Mandry<sup>3,4</sup> · Gilles Karcher<sup>1</sup> · Pierre-Yves Marie<sup>1,5</sup> · Antoine Verger<sup>1,3</sup>

Received: 18 June 2020 / Accepted: 11 August 2020 / Published online: 18 August 2020  
© Springer-Verlag GmbH Germany, part of Springer Nature 2020

## Abstract

**Purpose** CT signs that are evocative of lung COVID-19 infections have been extensively described, whereas  $^{18}\text{F}$ -FDG-PET signs have not. Our current study aimed to identify specific COVID-19  $^{18}\text{F}$ -FDG-PET signs in patients that were (i) suspected to have a lung infection based on  $^{18}\text{F}$ -FDG-PET/CT recorded during the COVID-19 outbreak and (ii) whose COVID-19 diagnosis was definitely established or excluded by appropriate viral testing.

**Methods** Twenty-two consecutive patients referred for routine  $^{18}\text{F}$ -FDG-PET/CT examinations during the COVID-19 outbreak (March 25th to May 15th 2020) and for whom CT slices were evocative of a lung infection were included in the study. All patients had undergone a SARS-COV-2 diagnostic test to confirm COVID-19 infection (positivity was based on molecular and/or serological tests) or exclude it (negativity of at least the serological test).

**Results** Eleven patients were confirmed to be affected by COVID-19 (COVID+), whereas the other eleven patients were not (COVID−) and were predominantly suspected of having bacterial pneumonia. CT abnormalities were not significantly different between COVID+ and COVID− groups, although trends toward larger CT abnormalities ( $p = 0.16$ ) and lower rates of consolidation patterns (0.09) were observed in the COVID+ group. The maximal standardized uptake values ( $\text{SUV}_{\text{max}}$ ) of lung areas with CT abnormalities were however significantly lower in the COVID+ than the COVID− group ( $3.7 \pm 1.9$  vs.  $6.9 \pm 4.1$ ,  $p = 0.03$ ), with the highest  $\text{SUV}_{\text{max}}$  consistently not associated with COVID-19.

**Conclusion** Among CT abnormalities evocative of lung infection, those related to COVID-19 are associated with a more limited  $^{18}\text{F}$ -FDG uptake. This observation may help improve our ability to detect COVID-19 patients.

**Keywords** COVID-19 ·  $^{18}\text{F}$ -FDG-PET · Lung infection · CT · Serological tests

## Introduction

Computed tomography (CT) abnormalities of the lung were described early during the COVID-19 outbreak [1] and have

provided considerable help in the diagnosis of COVID-19, especially prior to the development of viral tests [2]. This is in contrast to  $^{18}\text{F}$ -FDG-PET, for which no particular signs were described [3] with the exception of  $^{18}\text{F}$ -FDG-PET

---

This article is part of the Topical Collection on Infection and inflammation

**Electronic supplementary material** The online version of this article (<https://doi.org/10.1007/s00259-020-04999-1>) contains supplementary material, which is available to authorized users.

---

✉ Antoine Verger  
a.verger@chru-nancy.fr

<sup>1</sup> Lorraine University, Department of Nuclear Medicine and Nancyclotep Imaging Platform, CHRU Nancy, F-54000 Nancy, France

<sup>2</sup> Lorraine University, Department of Virology, CHRU Nancy, F-54000 Nancy, France

<sup>3</sup> Lorraine University, IADI, INSERM U1254, F-54000 Nancy, France

<sup>4</sup> Lorraine University, Department of Radiology, Brabois, CHRU Nancy, F-54000 Nancy, France

<sup>5</sup> Lorraine University, DCAC, INSERM U1116, F-54000 Nancy, France

confirmation of high pulmonary tropism in COVID-19 patients [4].

High rates of unexpected lung  $^{18}\text{F}$ -FDG-PET/CT abnormalities were reported during the outbreak [5, 6], but unfortunately, these abnormalities could not be unambiguously associated with a SARS-COV-2 infection in the absence of confirmation from a specific viral diagnostic assay.

It is now possible to use molecular reverse transcriptase-polymerase chain reaction (RT-PCR) tests in combination with serological assays to confirm a COVID-19 diagnosis (positivity of molecular and/or serological tests) or to exclude it (negativity of at least the serological assay) with a high diagnostic accuracy [7]. The event of a definitive COVID-19 diagnosis thereby allowed a precise description of  $^{18}\text{F}$ -FDG-PET abnormalities in COVID-19 patients.

Our current study aimed to identify specific COVID-19  $^{18}\text{F}$ -FDG-PET signs in patients for whom (i) lung infection was suspected from  $^{18}\text{F}$ -FDG-PET/CT recorded during the COVID-19 outbreak and (ii) COVID-19 diagnosis was definitively established or excluded by the appropriate viral testing.

## Methods

Between March 25 and May 15, 2020, 884 patients underwent  $^{18}\text{F}$ -FDG-PET examinations in our nuclear medicine department. Twenty-two of these patients (2.5%) were retrospectively selected on the basis of the presence of COVID-19 compatible CT abnormalities (e.g., ground-glass opacities, crazy-paving, and/or consolidation patterns), as determined by experienced observers (AB, CB, and AV). All patients examined in our hospital are informed that their medical data is anonymized prior to being used for research purposes.

Whole-body  $^{18}\text{F}$ -FDG-PET/CT was performed on a digital hybrid system (Vereos, Philips®) 1 h after injection of 3.5 MBq/kg of  $^{18}\text{F}$ -FDG and with a recording time of 90 s/step. All patients were asked to fast for at least 6 h prior to the PET examination, and all patients had a blood glucose level of < 180 mg/L at the time of the  $^{18}\text{F}$ -FDG injection. PET images were reconstructed with 2-mm isotropic voxels, an OSEM algorithm (3 iterations, 3 subsets) a recovery resolution method (PSF: 1 iteration and 6 mm regularization kernel), and further corrections for scatter, random, and attenuation. The CT scan parameters were as follows: 120 kV, iDose 4 with average mAs of 72, pitch 0.828, speed rotation 0.5 s, and slice thickness 2 mm/increment of 1.25 mm.

CT lung abnormalities that were evocative of COVID-19 were classified using the conventional nomenclature; ground-glass opacities (GGO), crazy-paving pattern (CPP), and consolidation (CON) [1]. Each pulmonary lobe was scored visually, according to the percentage of pulmonary involvement, and an extent score was determined for each patient by adding up the lobe scores [1]. Maximal standardized uptake values

( $\text{SUV}_{\text{max}}$ ) were used to measure the metabolic activity of lung areas with CT abnormalities. An  $\text{SUV}_{\text{max}}$  was determined for each individual patient irrespective of the type of lesion and in addition, for all areas of each of the different types of CT lesions (GGO, CPP, and CON).

In our department, serological testing was systematically prescribed for all patients exhibiting CT lung abnormalities evocative of COVID-19 on the  $^{18}\text{F}$ -FDG-PET/CT exams, which were routinely recorded during the COVID-19 outbreak, except for patients who had returned a previous positive molecular test result. A lateral flow immunoassay serologic test (BioSynex® IgM/IgG) was prescribed for this purpose because of its higher sensitivity compared with the SARS-COV-2 RT-PCR tests available at the time of the examination (i.e., at > 15 days from symptom onset).

Statistical analyses were performed with the SPSS-Statistics software (version 25.0), with  $p$ -values < 0.05 considered significant. Student  $t$  test was used to compare the means of quantitative variables, with adjustment in case of unequal variances determined by Levene's test and Chi-square tests for comparisons between two categorical variables.

## Results

### Analyses of the overall population

Among the 22 patients included in the study, 11 were finally identified as negative for SARS-COV-2 infection (COVID-group), on the basis of a negative serologic test result for both IgG and IgM in all cases (5 patients returned an additional and negative RT-PCR test). The other 11 patients were identified as positive by RT-PCR ( $n = 9$ ) or serological testing ( $n = 2$ ) (COVID+ group). COVID positivity was determined prior to the  $^{18}\text{F}$ -FDG-PET/CT scan in 7 COVID+ patients.

In COVID- patients, the final diagnosis, based on the subsequent follow-up, was granulomatosis in 2 cases (patients undergoing immunotherapy with clinical and radiological improvement after treatment), lymphoma in one case (recurrent non-Hodgkin's lymphoma), and bacterial pneumonia in the 8 remaining cases (clinical and radiological improvement after antibiotic treatment).

CT abnormalities observed included all 3 types of CT lesions (GGO, CPP, and CON) in 3 patients, only 2 types of CT lesions in 11 cases (6 CPPs with GGOs and 5 CPPs with CON patterns), and only one type of CT lesion in 8 patients (6 GGOs and 2 CON patterns). The  $\text{SUV}_{\text{max}}$  was strongly influenced by this CT classification with an increase in mean  $\text{SUV}_{\text{max}}$  being observed between the lung areas with GGOs ( $2.3 \pm 1.1$ ,  $n = 15$ ), CPPs ( $3.8 \pm 2.3$ ,  $n = 14$ ) and CON patterns ( $7.1 \pm 3.9$ ,  $n = 10$ ) ( $p < 0.001$ ) and with the mean  $\text{SUV}_{\text{max}}$  from CON areas specifically and markedly different than those from CPP or CGO areas ( $3.0 \pm 1.9$ ,  $p < 0.001$ ).

## Comparisons between COVID– and COVID+ patients

As detailed in Table 1, COVID+ patients presented a higher body mass index (BMI) than COVID– patients ( $p = 0.04$ ), as well as a non-significant trend toward older age ( $p = 0.09$ ), more extensive CT abnormalities ( $p = 0.16$ ), and lower rates of CT consolidation patterns ( $p = 0.12$ ). The  $SUV_{max}$  of the lung CT abnormalities were significantly lower in COVID+ than COVID– patients ( $3.7 \pm 1.9$  vs.  $6.9 \pm 4.1$ ,  $p = 0.03$ ). This difference remained significant when the comparison focused on the 39 lung areas corresponding to different patterns of CT abnormalities ( $3.0 \pm 1.7$  vs.  $5.2 \pm 3.8$ ,  $p = 0.03$ ), and this difference also remained perceptible when the analysis was solely restricted to CON areas, although it just fell short of the statistical significance threshold ( $3.7 \pm 2.1$  vs.  $8.6 \pm 3.6$ ,  $p = 0.07$ ). This difference was not observed in areas with GGOs or CPPs ( $2.9 \pm 1.7$  vs.  $3.2 \pm 2.2$ ,  $p = 0.67$ ).

Figure 1 further compares  $SUV_{max}$  lung CT abnormalities between COVID+ and COVID– patients as box plots showing individual values. No other significant  $^{18}F$ -FDG-PET finding was observed between the 2 patient's groups (Supplemental Table).

Two representative PET-CT images of a COVID+ and COVID– patient are shown in Fig. 2.

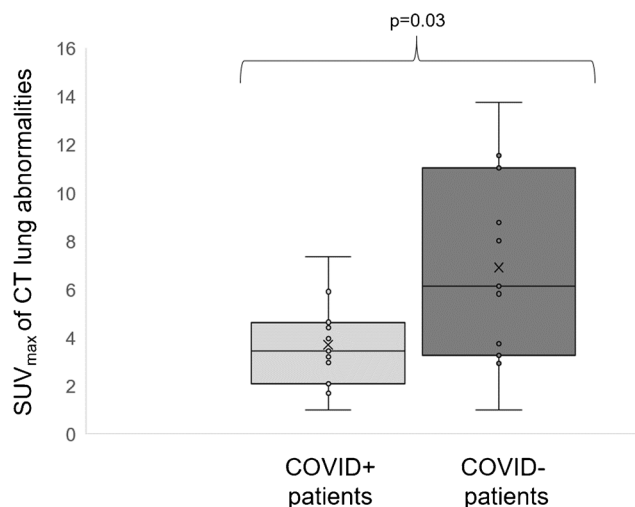


**Fig. 1** Box plots of  $SUV_{max}$  measurements of CT lung abnormalities in COVID+ and COVID– patients

## Discussion

There was an increased prevalence of  $^{18}F$ -FDG PET-CT abnormalities evocative of a lung infection, during the COVID-19 outbreak [4, 5]. Thanks to viral test procedures allowing to definitively exclude or confirm a COVID-19 diagnosis, the present study shows that a great proportion of such suspected

**Table 1** Comparison of patients' characteristics and imaging results between the presence (COVID+) and absence (COVID–) of a SARS-COV-2 infection

	COVID+ (n = 11)	COVID– (n = 11)	P value
18F-FDG PET indications			0.03*
Initial diagnosis or follow-up of a cancer	4 (36%)	10 (91%)	
Suspicion of prosthesis infection, vasculitis, or endocarditis	4 (36%)	1 (9%)	
Part of workups of macrophage activation syndrome or pericarditis	3 (28%)	–	
Age (years)	72 ± 10	62 ± 15	0.09
Female gender	4 (36%)	2 (18%)	0.34
Body mass index (kg.m <sup>-2</sup> )	27.7 ± 5.8	23.3 ± 3.3	0.04*
Infectious symptoms	8 (73%)	8 (73%)	1.00
Delay from symptom onset (days)	12 ± 5	11 ± 6	0.80
C-Reactive Protein (mg.L <sup>-1</sup> ) <sup>‡</sup>	36.8 ± 37.8	133.6 ± 139.3	0.20
Extent of CT lung abnormality score	11.5 ± 8.0	6.7 ± 7.2	0.16
Presence of a GGO pattern by CT	8 (73%)	7 (64%)	0.65
Presence of a CPP pattern by CT	7 (64%)	7 (64%)	1.00
Presence of a CON pattern by CT	3 (27%)	7 (64%)	0.09
$SUV_{max}$ of lung CT abnormalities	3.7 ± 1.9	6.9 ± 4.1	0.03*
$SUV_{max}$ in areas with CON, GGO or CPP lesions (n = 20/n = 19)	3.0 ± 1.7	5.2 ± 3.8	0.03*
$SUV_{max}$ in areas with CON lesions (n = 3/n = 7)	3.7 ± 2.1	8.6 ± 3.6	0.07
$SUV_{max}$ in areas with GGO or CPP lesions (n = 17/n = 12)	2.9 ± 1.7	3.2 ± 2.2	0.67

\*:  $p < 0.05$  for the comparison between COVID+ and COVID– patients

<sup>‡</sup> C-Reactive Protein (mg.L<sup>-1</sup>): C-Reactive Protein only available for 12 patients (7 COVID+ and 5 COVID–)

BMI: Body mass index; CON: pattern of consolidation by CT; GGO: pattern of Ground Glass Opacity by CT; CPP: Crazy-Paving pattern by CT;  $SUV_{max}$ : maximal standardized uptake value

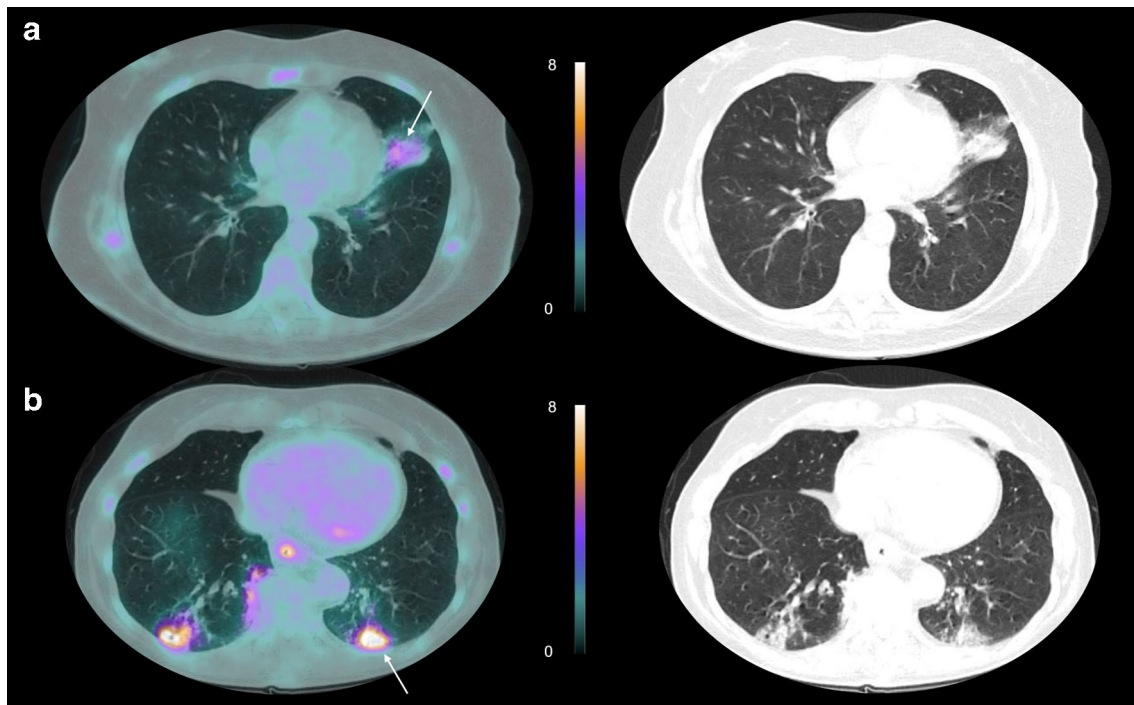


**Fig. 2** Representative examples of CT lung abnormalities on axial slices of  $^{18}\text{F}$ -FDG-PET in (a) a 61-year-old-woman with a COVID-19 positive RT-PCR test ( $\text{SUV}_{\text{max}}$  of 4.4 for the lung CT condensation associated with a crazy-paving pattern, shown by white arrow) and (b) in a 74-year-

old-woman with a negative COVID-19 serological test and a final diagnosis of bacterial pneumonia ( $\text{SUV}_{\text{max}}$  at 8.0 for the lung CT condensation, associated with a crazy-paving pattern, shown by white arrow)

lung infections are unequivocally associated with a SARS-COV-2 infection (i.e., one half of the cases examined).

Molecular RT-PCR positivity may be documented early in symptomatic COVID-19 patients but is variable and may disappear after 1 month or a little more [2]. Conversely, serological tests are positive for a longer time period, but the appearance of this positivity is delayed due to seroconversion and generally only occurs after the 10th day of the onset of symptoms [2]. A combination of molecular and serological tests, as applied in the present study, is therefore required to confirm or exclude SARS-COV-2 infections.

The lower  $\text{SUV}_{\text{max}}$  observed in the lungs of our COVID-19 patients is likely explained by a combination of several factors among which a trend toward lower rates of CT consolidation patterns in COVID+ (27%) than in COVID- (64%) patients. Indeed, areas with consolidation patterns were associated with much higher  $\text{SUV}_{\text{max}}$  values when compared with areas exhibiting ground-glass opacities or crazy paving patterns, which is consistent with previous reports in certain inflammatory pneumoniae [8]. Ground-glass opacities and crazy-paving patterns include a non-cellular component, particularly in fluid filled intra-alveolar regions [9], which are less likely to take up FDG.

The  $\text{SUV}_{\text{max}}$  in areas with consolidation patterns were also seemingly lower in COVID+ than in COVID- patients (Table 1). This may be because the tissue changes related to COVID-19 are not simply restricted to an infectious and inflammatory cell infiltrate with in particular, the subsequent

occurrence of various vascular-related damage, i.e., capillary leakage and vessel thrombosis [10]. If confirmed by further studies, this observation would be particularly informative because the consolidation pattern is predominantly observed in bacterial pneumonia, which is the major alternative diagnosis.

The main limitations of our study are inherently due to its small retrospective observational design. Our results therefore require further confirmation on a much larger scale.

From a more practical clinical standpoint, our results strengthen the notion than CT abnormalities evocative of COVID-19 are far from specific. Our results do however provide specific evidence that a COVID-19 diagnosis is unlikely if these CT abnormalities are associated with high  $\text{SUV}_{\text{max}}$  levels by  $^{18}\text{F}$ -FDG-PET. Despite this positive finding, there remains significant overlap of  $\text{SUV}_{\text{max}}$  values between COVID+ and COVID- patients, and, therefore, gold standard diagnostics should still apply. In addition, further multicenter studies are required to evaluate the predictive benefits of this finding and to optimize thresholds as a function of the  $^{18}\text{F}$ -FDG-PET recording and reconstruction parameters used.

**Availability of data and material** The data that support the findings of this study are available on request from the corresponding author (AV).

**Authors' contributions** All authors contributed significantly to the analysis and interpretation of the data (AB, CB, HJ, PYM, AV), to the writing of the manuscript (AB, PYM, AV), and to the revision of the manuscript (LI, DM, PO, GK, AV).

## Compliance with ethical standards

**Conflicts of interest/competing interests** The authors disclose no potential conflicts of interest related to the present work.

**Ethics approval and consent to participate** All procedures performed in studies involving human participants were in accordance with the ethical standards of the institutional and/or national research committees and with the 1964 Helsinki declaration and its latest amendments or comparable ethics standards. All patients that participated in the study provided their informed consent, and the study was approved by the local Ethics Committee (Comité éthique du CHRU Nancy).

**Consent for publication** Not applicable

**Code availability** Not applicable.

## References

- Pan F, Ye T, Sun P, Gui S, Liang B, Li L, et al. Time course of lung changes at chest CT during recovery from coronavirus disease 2019 (COVID-19). *Radiology*. 2020;295(3):715–21.
- Carter LJ, Garner LV, Smoot JW, Li Y, Zhou Q, Saveson CJ, et al. Assay Techniques and Test Development for COVID-19 Diagnosis. *ACS Cent Sci*. 2020;6(5):591–605.
- Guedj E, Verger A, Cammilleri S. PET imaging of COVID-19: the target and the number. *Eur J Nucl Med Mol Imaging*. 2020;47(7):1636–7.
- Qin C, Liu F, Yen T-C, Lan X. 18F-FDG PET/CT findings of COVID-19: a series of four highly suspected cases. *Eur J Nucl Med Mol Imaging*. 2020;47(5):1281–6.
- Albano D, Bertagna F, Bertoli M, Bosio G, Lucchini S, Motta F, et al. Incidental findings suggestive of COVID-19 in asymptomatic patients undergoing nuclear medicine procedures in a high-prevalence region. *J Nucl Med*. 2020;61(5):632–6.
- Setti L, Kirienko M, Dalto SC, Bonacina M, Bombardieri E. FDG-PET/CT findings highly suspicious for COVID-19 in an Italian case series of asymptomatic patients. *Eur J Nucl Med Mol Imaging*. 2020;47(7):1649–56.
- Sethuraman N, Jeremiah SS, Ryo A. Interpreting Diagnostic Tests for SARS-CoV-2. *JAMA*. 2020;323(22):2249.
- Tateishi U, Hasegawa T, Seki K, Terauchi T, Moriyama N, Arai Y. Disease activity and 18F-FDG uptake in organising pneumonia: semi-quantitative evaluation using computed tomography and positron emission tomography. *Eur J Nucl Med Mol Imaging*. 2006;33(8):906–12.
- Schaller T, Hirschtbühl K, Burkhardt K, Braun G, Trepel M, Märkl B, et al. Postmortem Examination of Patients With COVID-19. *JAMA*. 2020 [cité 15 juin 2020]; Disponible sur: <https://jamanetwork.com/journals/jama/fullarticle/2766557>
- Iba T, Levy JH, Levi M, Connors JM, Thachil J. Coagulopathy of Coronavirus Disease 2019. *Crit Care Med*. 2020 [cité 15 juin 2020]. Disponible sur: <https://journals.lww.com/10.1097/CCM.0000000000004458>

**Publisher's note** Springer Nature remains neutral with regard to jurisdictional claims in published maps and institutional affiliations.